Orbital-free density functional theory: Kinetic potentials and *ab initio* local pseudopotentials

Jeng-Da Chai[1,*] and John D. Weeks[1,2]
[1]*Institute for Physical Science and Technology, University of Maryland, College Park, Maryland 20742, USA*
[2]*Department of Chemistry and Biochemistry, University of Maryland, College Park, Maryland 20742, USA*
(Received 6 January 2007; revised manuscript received 20 March 2007; published 23 May 2007)

In the density functional (DF) theory of Kohn and Sham, the kinetic energy of the ground state of a system of noninteracting electrons in a general external field is calculated using a set of orbitals. Orbital-free methods attempt to calculate this directly from the electron density by approximating the universal but unknown kinetic energy density functional. However, simple local approximations are inaccurate, and it has proven very difficult to devise generally accurate nonlocal approximations. We focus instead on the kinetic potential, the functional derivative of the kinetic energy DF, which appears in the Euler equation for the electron density. We argue that the kinetic potential is more local and more amenable to simple physically motivated approximations in many relevant cases, and describe two pathways by which the value of the kinetic energy can be efficiently calculated. We propose two nonlocal orbital free kinetic potentials that reduce to known exact forms for both slowly varying and rapidly varying perturbations and also reproduce exact results for the linear response of the density of the homogeneous system to small perturbations. A simple and systematic approach for generating accurate and weak *ab initio* local pseudopotentials which produce a smooth slowly varying valence component of the electron density is proposed for use in orbital-free DF calculations of molecules and solids. The use of these local pseudopotentials further minimizes the possible errors from the kinetic potentials. Our theory yields results for the total energies and ionization energies of atoms, and for the shell structure in the atomic radial density profiles that are in very good agreement with calculations using the full Kohn-Sham theory.

DOI: 10.1103/PhysRevB.75.205122 PACS number(s): 71.15.Mb, 71.15.Dx, 31.15.Ew

I. INTRODUCTION

Density functional theory (DFT) has become one of the most powerful tools for investigating the electronic structure of large complex systems. In principle, as shown by Hohenberg and Kohn,[1] the exact ground-state energy of a system of N electrons can be formally written as a functional $E[\rho]$ of only the electron density $\rho(\mathbf{r})$, a function of three variables, and the external field $V_{\text{ext}}(\mathbf{r})$. Determining the energy and other ground-state properties from such an approach could dramatically reduce the computational cost for large systems when compared with traditional quantum chemistry methods, which deal with wave functions involving coordinates of all N electrons.[2,3]

Kohn and Sham (KS)[4,5] showed that $E[\rho]$ can be usefully partitioned into the following set of terms:

$$E[\rho] = T_s[\rho] + E_H[\rho] + E_{\text{xc}}[\rho] + \int \rho(\mathbf{r}) V_{\text{ext}}(\mathbf{r}) d\mathbf{r}. \quad (1)$$

Here $T_s[\rho]$ is the noninteracting kinetic energy density functional (KEDF), which gives the kinetic energy of a model system of N noninteracting electrons in a self-consistent-field chosen so that the ground-state density equals $\rho(\mathbf{r})$,

$$E_H[\rho] \equiv \frac{1}{2} \int \int \frac{\rho(\mathbf{r})\rho(\mathbf{r}')}{|\mathbf{r}-\mathbf{r}'|} d\mathbf{r} d\mathbf{r}' \quad (2)$$

is the classical electron-electron potential energy (Hartree energy) and $E_{\text{xc}}[\rho]$ is the exchange-correlation energy (including the difference between the interacting and noninteracting kinetic energy and the difference between the quantum and classical electron-electron potential energy). The last term on the right-hand side of Eq. (1) is the only term that depends explicitly on the external potential $V_{\text{ext}}(\mathbf{r})$. Atomic units are used throughout the paper.

If all these functionals were known, then the density $\rho(\mathbf{r})$ could be obtained from the variational principle (Euler equation) associated with minimizing Eq. (1),

$$\mu = V_{T_s}(\mathbf{r};[\rho]) + V_{\text{eff}}(\mathbf{r};[\rho]), \quad (3)$$

and the total energy of the inhomogeneous system could then be determined from the energy functional $E[\rho]$. All other physical quantities related to the ground-state density could also be computed. Here μ is the chemical potential [the Lagrange multiplier associated with the normalization condition $\int \rho(\mathbf{r}) d\mathbf{r} = N$], and $V_{\text{eff}}(\mathbf{r};[\rho])$ is an effective one-body potential defined by

$$V_{\text{eff}}(\mathbf{r};[\rho]) \equiv \frac{\delta}{\delta\rho(\mathbf{r})} \left\{ E_H[\rho] + E_{\text{xc}}[\rho] + \int \rho(\mathbf{r}) V_{\text{ext}}(\mathbf{r}) d\mathbf{r} \right\}$$
$$= V_H(\mathbf{r};[\rho]) + V_{\text{xc}}(\mathbf{r};[\rho]) + V_{\text{ext}}(\mathbf{r}), \quad (4)$$

where

$$V_H(\mathbf{r};[\rho]) \equiv \delta E_H[\rho]/\delta\rho(\mathbf{r}) = \int \frac{\rho(\mathbf{r}')}{|\mathbf{r}-\mathbf{r}'|} d\mathbf{r}' \quad (5)$$

is the Hartree potential, and $V_{\text{xc}}(\mathbf{r};[\rho]) \equiv \delta E_{\text{xc}}[\rho]/\delta\rho(\mathbf{r})$ is the exchange-correlation potential. Similarly, we interpret

$$V_{T_s}(\mathbf{r};[\rho]) \equiv \delta T_s[\rho]/\delta\rho(\mathbf{r}) \quad (6)$$

as the kinetic potential (KP) arising from the KEDF.[6]

Further progress requires an accurate determination of the noninteracting kinetic energy, whose magnitude is much larger than the exchange-correlation energy. The initial development of DFT as a practical computational method was

made possible by KS's realization that the numerical value of the noninteracting kinetic energy can be exactly calculated, not directly from the density itself using $T_s[\rho]$, but by introducing a set of N one-electron wave functions (orbitals) satisfying the N coupled KS equations that describe the model system.[4,5]

Research could then focus on determining the remaining small term $E_{xc}[\rho]$. Here even local density approximations have often proved useful. Through the efforts of many workers, we now have generally accurate expressions for $E_{xc}[\rho]$. Using these along with the KS orbitals to calculate the kinetic energy, one can accurately calculate both the total energy $E[\rho]$ and the ground-state density $\rho(\mathbf{r})$ for a wide variety of systems.

However, the use of the KS orbitals usually generates a relatively expensive $O(N^3)$ scaling of computational cost with the number of electrons. While this scaling is much better than that of most standard methods that include correlation energy, calculations for large systems remain problematic. This remaining bottleneck could be removed if there were an accurate treatment of the kinetic energy in terms of the electron density only.[2,3,7]

To that end, there has been considerable effort invested in developing "orbital-free" density functional theory (OF-DFT) by making direct approximations for $T_s[\rho]$.[8–20] While earlier simple local density approximations for $T_s[\rho]$ like those used in the Thomas-Fermi (TF) model[21] are very inaccurate, there have been two main advances in recent work that offer prospects for significant improvements.

The first is the introduction of nonlocal KEDFs that reproduce known exact results for very slowly varying or very rapidly varying fields and give the exact linear response (LR) of the density of the uniform model system to small perturbations. Similar ideas have been successfully applied to classical nonuniform fluids.[22] The second advance is to focus not on the total density but on the smaller and more slowly varying valence electron density as described by a weak pseudopotential acting only on the valence electrons. While conventional pseudopotential methods use orbitals, recently developed *ab initio* local pseudopotential (AILPS) methods determine the unique local one-body potential producing a given target valence density by solving the KS equations inversely, using the one-to-one mapping between density and potentials in DFT.[23] For OF-DFT with LR-based KEDF's, the use of pseudopotentials not only can reduce the computational cost, but also can improve its accuracy, since the system will be closer to the LR regime where $T_s[\rho]$ is designed to be accurate.[24,25] Indeed, very promising results using such OF-DFT methods have been obtained for a variety of nearly free-electron-like metals.

However, existing KEDF's have not yet achieved chemical accuracy for systems with localized and more rapidly varying electron densities like molecules or for covalent or ionic solids. The main problem is that the exact $T_s[\rho]$ is highly nonlocal, and we have little idea of the functional form of the nonlocality for densities far from the LR regime. It has proven very difficult to understand what errors an approximate nonlocal $T_s[\rho]$ will produce in the density as determined by the Euler equation with a general $V_{ext}(\mathbf{r})$.

We explore here a different way to attack this basic problem. The exact $T_s[\rho]$ can be formally obtained from $V_{T_s}(\mathbf{r};[\rho])$ by functional integration over density changes in all regions of space.[6,18] Because of this integration $T_s[\rho]$ is a more nonlocal functional of the density than is $V_{T_s}(\mathbf{r};[\rho])$. More detailed arguments arriving at this same conclusion have been recently presented.[26] Since most problems in devising accurate approximations for $T_s[\rho]$ have arisen from the nonlocality, this suggests it could be worthwhile to try to develop approximations for the KP $V_{T_s}(\mathbf{r};[\rho])$ itself.

To illustrate this point, Chai and Weeks[7] added a simple gradient correction to the original local TF KP for atoms,[21] with a coefficient chosen to reproduce the exact boundary condition of exponential decay of the electron density far from the nucleus. Though quantitative results were not obtained, the resulting modified Thomas-Fermi (MTF) model gave energies for atoms and for closed-shell diatomic molecules that showed notable improvements when compared to the original TF and related gradient corrected KEDF models. However, the local gradient correction used in the MTF KP cannot reproduce the oscillatory atomic shell structure, and it does not satisfy the exact LR behavior in the homogeneous limit. It is clear that nonlocality even in the KP must be taken into account to achieve more accurate results.

We propose here nonlocal approximations for the KP using ideas similar to those employed for the nonlocal KEDFs. These KPs satisfy the exact LR condition in the uniform limit, and reproduce known exact limiting forms of $V_{T_s}(\mathbf{r};[\rho])$ both for very slowly varying and very rapidly varying perturbations. As will become clear, the nonlocality in our KP is determined by the requirement that LR is exactly satisfied, and it is much easier to ensure that LR holds for the KP than it is for analogous KEDF models. We believe this level of nonlocality in the KP may suffice in many cases when used in conjunction with AILPS methods to describe slowly varying valence density components closer to the LR regime.

The remainder of this paper is organized as follows. Section II will discuss some general pathways connecting $T_s[\rho]$ and $V_{T_s}(\mathbf{r};[\rho])$. Section III will describe limiting forms of the KEDF and KP for slowly varying and rapidly varying perturbations, and discuss LR theory, an exact theory for the response of density of the uniform electron gas to small perturbations. Section IV will develop two nonlocal KPs incorporating both the correct limiting forms of the exact KP and the exact LR of the free-electron gas. Section V will compare the numerical results of the present method for atoms with the KS-DFT and other KEDFs, both for all-electron calculations and for valence electrons using the AILPS. We find that the use of AILPS indeed reduces errors arising from nonlocality in these approximate KPs or KEDFs, which give very accurate results for the relatively slowly varying valence densities. Our conclusions are given in Sec. VI.

II. PATHWAYS FROM $V_{T_s}(\mathbf{r};[\rho])$ TO $T_s[\rho]$

If $T_s[\rho]$ is known, $V_{T_s}(\mathbf{r};[\rho])$ can be simply computed by functional differentiation. However, there is no unique way

of determining $T_s[\rho]$ from a given $V_{T_s}(\mathbf{r};[\rho])$. Many possible pathways can be used to construct $T_s[\rho]$ by functional integration of $V_{T_s}(\mathbf{r};[\rho])$.[27,28] If the exact $V_{T_s}(\mathbf{r};[\rho])$ is used and the integration is carried out exactly, then all pathways would give the same exact result for $T_s[\rho]$. However, when an approximate $V_{T_s}(\mathbf{r};[\rho])$ is used, different pathways will give different results for the kinetic energy. But this "thermodynamic inconsistency" is small if reasonably good approximations are used, since the integration tends to smooth out local errors that may exist in the density.[7,28]

More problematic is the fact that most pathways require additional results for partially coupled systems as the external field or density perturbation is gradually turned on, which adds to the computational burden. In particular, most earlier work has used a "potential energy pathway," where the external potential is scaled by a coupling parameter.[7,27] The kinetic energy can then be found by subtracting the potential energy (calculated from the potential energy density functionals) from the total energy. However, this pathway is expensive, since one must solve the Euler equation (3) for each partially coupled $V_{\text{ext}}^{\lambda}(\mathbf{r})$ (with the same μ), to determine the corresponding ρ_λ.

A. Herring's pathway

However, Herring showed there is a particular pathway arising from exact scaling relations between the noninteracting kinetic energy $T_s[\rho]$ with respect to the coordinate $\mathbf{r}$ in $\rho(\mathbf{r})$ where very simple results involving only the final density can sometimes be found.[6,18] If the coordinate $\mathbf{r}$ is scaled to $\alpha\mathbf{r}$, the normalized scaled density is $\rho_\alpha(\mathbf{r})=\alpha^3\rho(\alpha\mathbf{r})$. It is easy to show that the exact $T_s[\rho]$ then obeys

$$\alpha^2 T_s[\rho] = T_s[\rho_\alpha]. \tag{7}$$

For isolated systems, such as atoms and molecules, the density and its derivatives to all order vanish far from the nuclei. For such systems, when Eq. (7) is differentiated with respect to α, and the partial derivative is evaluated at $\alpha=1$, we find the formally exact result

$$T_s[\rho] = \frac{1}{2}\int V_{T_s}(\mathbf{r};[\rho])\,\boldsymbol{\nabla}\cdot(\mathbf{r}\rho(\mathbf{r}))d\mathbf{r}. \tag{8}$$

Therefore, once the kinetic potential $V_{T_s}(\mathbf{r};[\rho])$ is known for some given $\rho(\mathbf{r})$, the numerical value of $T_s[\rho]$ can then be immediately determined from Eq. (8). Since there is no need to perform a coupling parameter integration over the change of density or potential, this scheme is not only fast, but also numerically reliable. The final form of Eq. (8) is essentially the viral theorem, and is directly related to the force on molecules.[29–32]

Note that this simple and exact pathway holds only for the *noninteracting* $T_s[\rho]$,[31] which again shows the virtues of the KS partitioning of the total energy. We will use Eq. (8) as the basic pathway to determine the numerical value of $T_s[\rho]$ from a given approximate $V_{T_s}(\mathbf{r};[\rho])$ for most calculations in this paper. However, Eq. (8) does not hold for extended solid-state systems because of nonvanishing boundary terms, and thus far we have not found an exact and simple way of including them.

Fortunately, there is another class of computationally efficient "density pathways" that can be used for extended systems, as we now show. Density pathways can also be used for atomic and molecular systems to check the accuracy of the V_{T_s} used, since results using the exact V_{T_s} would be independent of path.[27,28]

B. Density pathways

The change in the kinetic energy can be formally related to a coupling parameter integration, where the density changes from some known value at $\lambda=0$ to the final density at $\lambda=1$,

$$T_s[\rho] = T_{\lambda=0} + \int_0^1 d\lambda \int d\mathbf{r} V_{T_s}(\mathbf{r};[\rho_\lambda])\frac{\partial\rho_\lambda(\mathbf{r})}{\partial\lambda}. \tag{9}$$

In most cases, a simple linear density pathway will suffice. Here the density $\rho(\mathbf{r})$ is linearly scaled by a coupling parameter λ from some uniform reference density ρ_0 naturally chosen to be the uniform electron density N/V in extended systems,

$$\rho_\lambda(\mathbf{r}) = \rho_0 + \lambda[\rho(\mathbf{r}) - \rho_0]. \tag{10}$$

Then Eq. (9) becomes

$$T_s[\rho] = T_{\lambda=0} + \int_0^1 d\lambda \int d\mathbf{r} V_{T_s}(\mathbf{r};[\rho_\lambda])[\rho(\mathbf{r}) - \rho_0]. \tag{11}$$

Here $T_{\lambda=0}$ is the kinetic energy of the uniform system, i.e., the Thomas-Fermi kinetic energy $T_{\text{TF}}[\rho_0]$. For extended systems, where the Herring's pathway cannot be used, this density pathway appears to be a good way to compute T. Other density pathways, such as the square-root pathway introduced by Chen and Weeks[28] to describe nonuniform hard sphere fluids, can be defined, and have proven to be useful in certain applications, but we do not consider them here.

Note from Eq. (10) that $\rho_\lambda(\mathbf{r})$ depends only on the final density, so evaluation of Eq. (11) is straightforward and this pathway is computationally efficient. Unlike the potential energy pathway where the external potential is scaled, there is no need to solve the Euler equation (3) for its corresponding external potential $V_{\text{ext}}^{\lambda}(\mathbf{r})$ at each λ. However, for isolated systems, where $\rho_0=0$, this pathway is likely to be less accurate than Herring's pathway, since it does not automatically satisfy the virial theorem.

III. EXACT LIMITS AND LINEAR RESPONSE THEORY

Although the exact $T_s[\rho]$ is still unknown, several limiting forms have been discovered for particular density distributions. These provide important cornerstones that can be used to construct accurate KEDFs and KPs in many cases, as will be seen below.

In particular, the Thomas-Fermi (TF) KEDF (Ref. 21) is known to be exact for a uniform system,

$$T_{\mathrm{TF}}[\rho] = C_F \int \rho^{5/3}(\mathbf{r}) d\mathbf{r}, \tag{12}$$

where $C_F = \frac{3}{10}(3\pi^2)^{2/3}$. The TF KEDF $T_{\mathrm{TF}}[\rho]$ is derived by local use of the uniform free-electron gas model, and is exact for a system with an infinite number of electrons. The corresponding expression for the TF KP is

$$V_{\mathrm{TF}}(\mathbf{r};[\rho]) \equiv \delta T_{\mathrm{TF}}[\rho]/\delta\rho(\mathbf{r}) = \tfrac{5}{3} C_F \rho^{2/3}(\mathbf{r}). \tag{13}$$

This depends only on the local value of $\rho^{2/3}(\mathbf{r})$ and thus formally is more local than the TF KEDF, whose functional dependence on ρ involves the density at all $\mathbf{r}$. Of course in this simple case, the functional integration of Eq. (13) can be carried out exactly to yield Eq. (12), but this cannot be done in general and the nonlocality of $T_s[\rho]$ has proved problematic.

Results for nonuniform systems are best described in Fourier space. For a very slowly varying perturbation, of the density, the second-order gradient expansion is exact.[33] It is easy to see that results correct to second order at small wave vectors are given by

$$T_{\mathrm{TF}(1/9)\mathrm{W}}[\rho] \equiv T_{\mathrm{TF}}[\rho] + \tfrac{1}{9} T_{\mathrm{W}}[\rho], \tag{14}$$

where

$$T_{\mathrm{W}}[\rho] \equiv \frac{1}{8} \int \frac{|\nabla\rho(\mathbf{r})|^2}{\rho(\mathbf{r})} d\mathbf{r} \tag{15}$$

is the von Weizsäcker (W) KEDF.[34]

$T_{\mathrm{W}}[\rho]$ is exact for a system with one or two electrons, or where the density can be accurately described by a single orbital. Moreover, it has been argued[8–10,12] that $T_{\mathrm{W}}[\rho]$ gives the correct leading order term for a rapidly varying perturbation with only high wave-vector components and that the next order correction is reproduced by

$$T_{\mathrm{W}-(3/5)\mathrm{TF}}[\rho] \equiv T_{\mathrm{W}}[\rho] - \tfrac{3}{5} T_{\mathrm{TF}}[\rho]. \tag{16}$$

The W KP is

$$V_{\mathrm{W}}(\mathbf{r};[\rho]) \equiv \delta T_{\mathrm{W}}[\rho]/\delta\rho(\mathbf{r}) = \frac{1}{8}\left(\frac{|\nabla\rho(\mathbf{r})|^2}{\rho^2(\mathbf{r})} - 2\frac{\nabla^2\rho(\mathbf{r})}{\rho(\mathbf{r})} \right). \tag{17}$$

If we represent the full density by an effective single orbital function $\psi(\mathbf{r})$,

$$\rho(\mathbf{r}) = |\psi(\mathbf{r})|^2, \tag{18}$$

then the W KP can be written in a compact form that will later prove useful,

$$V_{\mathrm{W}}(\mathbf{r};[\rho]) = -\frac{\nabla^2\psi(\mathbf{r})}{2\psi(\mathbf{r})}. \tag{19}$$

Finally, the linear response of the density of a uniform noninteracting electron gas with density ρ_0 to a small perturbation $\delta V(\mathbf{k}) = \epsilon_{\mathbf{k}} e^{i\mathbf{k}\cdot\mathbf{r}}$ is exactly known,[35]

$$\delta\rho(\mathbf{k}) = \chi_L(q)\, \delta V(\mathbf{k}). \tag{20}$$

Here

$$q \equiv k/2k_F \tag{21}$$

is a dimensionless wave vector, where

$$k_F \equiv (3\pi^2\rho_0)^{1/3} \tag{22}$$

is the Fermi wave vector (FWV) and $k \equiv |\mathbf{k}|$. The LR function $\chi_L(q)$ has the form

$$\chi_L(q) = -\frac{k_F}{\pi^2} F_L^{-1}(q) = -\frac{k_F}{\pi^2}\left[\frac{1}{2} + \frac{1-q^2}{4q} \ln\left| \frac{1+q}{1-q} \right| \right], \tag{23}$$

where

$$F_L(q) \equiv \left[\frac{1}{2} + \frac{1-q^2}{4q} \ln\left| \frac{1+q}{1-q} \right| \right]^{-1} \tag{24}$$

has been called the Lindhard function.[10]

It is known that the weak logarithmic singularity at $q=1$ in $F_L^{-1}(q)$ is responsible for Friedel oscillations, and may also be important for the appearance of atomic shell structure. This singularity further divides the Lindhard function into two branches in Fourier space: the low-momentum ($q<1$) or the low-q (LQ) branch, and the high-momentum ($q>1$) or the high-q (HQ) branch.[10]

The dimensionless response function arising from the TF KEDF is $F_{\mathrm{TF}}(q)=1$, and that from the W KEDF is $F_{\mathrm{W}}(q)=3q^2$.[36] Clearly, no linear combination of the TF and the W KEDFs can reproduce the exact Lindhard function in Eq. (24). This has the following two limits:[10]

$$F_L(q) = \begin{cases} 1 + q^2/3 + O(q^4), & q \ll 1, \\ 3q^2 - 3/5 + O(q^{-2}), & q \gg 1. \end{cases} \tag{25}$$

It should be noted that the expansions for both the low-q and high-q limits are correct to all orders in perturbation theory, but valid only in the appropriate limits in Fourier space. On the other hand, the LR theory is valid for all wave vectors, but is only accurate for small perturbations. Therefore, the regime where the response functions of the two limiting KEDFs deviate from the exact LR function gives an indication of the range of wave vectors where the two limiting forms are inaccurate.

As shown in Fig. 1, the response function $F_{\mathrm{TF}}^{-1}(q)$ has no momentum dependence and is only exact at $q=0$. The response function $F_{\mathrm{W}}^{-1}(q)$ is exact asymptotically at high q, and remains fairly accurate for $q \gtrsim 2$, but is divergent in the low-q branch, and fails completely for the nearly uniform electron gas. In contrast, the MTF model[7] gives a reasonably accurate average description of the exact response function, especially in the important region near the singularity at $q=1$.

IV. CONSTRUCTION OF NONLOCAL KINETIC POTENTIALS

A. Kinetic energy density functionals $T_{\mathrm{TF}\lambda\mathrm{W}}[\rho]$ and $T_{\mathrm{W}\lambda\mathrm{TF}}[\rho]$

Simple linear combinations of the two limiting KEDF's in Eqs. (12) and (15), such as the TFλW KEDF,[33,37–39]

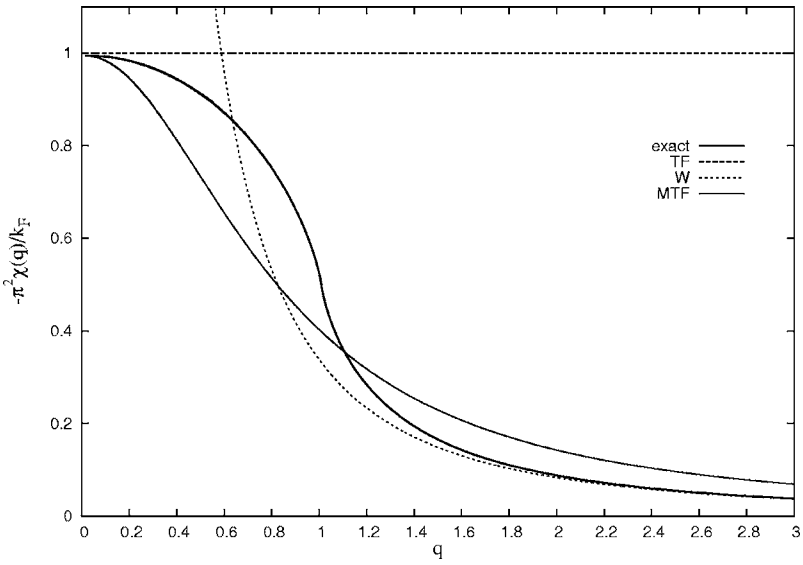

FIG. 1. Linear response functions of a uniform system of noninteracting fermions as given by the TF, W, and MTF (see Ref. 7) models.

$$T_{\mathrm{TF}\lambda\mathrm{W}}[\rho] \equiv T_{\mathrm{TF}}[\rho] + \lambda T_w[\rho], \tag{26}$$

and the WλTF KEDF,[40–43]

$$T_{\mathrm{W}\lambda\mathrm{TF}}[\rho] \equiv T_{\mathrm{W}}[\rho] + \lambda T_{\mathrm{TF}}[\rho], \tag{27}$$

have been widely studied for several decades. The value of the parameter λ was either determined empirically for getting good atomic energy or obtained by some semiclassical arguments.

The advantage of these approaches is the ability to generate a family of simple KEDF's easily. It has been shown empirically that the TF1/5W model can give good values for atomic energies, but the predicted density profiles are generally not very accurate, both near and far away from the nucleus. The $T_{\mathrm{TF}\lambda\mathrm{W}}[\rho]$ and $T_{\mathrm{W}\lambda\mathrm{TF}}[\rho]$ functionals give the correct leading term in the density response to a slowly-varying perturbation, and a rapidly-varying perturbation, respectively, and with particular choices of λ as in Eqs. (14) and (16) they can reproduce the next order term. Unfortunately, they then will have an incorrect leading term in the opposite limit, unless $\lambda=1$. However, it has been shown that $T_{\mathrm{TFW}}[\rho]$ with $\lambda=1$ always overestimates the exact $T_s[\rho]$ for various systems.[10] Finally, none of these functionals can reproduce the exact response function $F_L(q)$ in the homogeneous limit. Since these models fail to satisfy all the known limits, and nonlocality in $T_s[\rho]$ is not correctly described, it is also not surprising that atomic shell structure is missing in these approaches.

B. Combining TF and W kinetic potentials

We argue that it may be more profitable to take advantage of known limiting forms of the KP, rather than the KEDF, and develop approximations for the more local $V_{T_s}(\mathbf{r};[\rho])$ directly. Again, we can rely on known results in the linear response regime when the density variations are not too large.

From Eqs. (14) and (16), the following linear combinations of the TF KP and the W KP in Eqs. (13) and (17) can reproduce exact results to second order for very small and very large wave-vector perturbations, respectively,

$$V_{T_s}(\mathbf{r};[\rho]) \approx \begin{cases} V_{\mathrm{TF}}(\mathbf{r};[\rho]) + \frac{1}{9}V_{\mathrm{W}}(\mathbf{r};[\rho]), & q \ll 1, \\ V_{\mathrm{W}}(\mathbf{r};[\rho]) - \frac{3}{5}V_{\mathrm{TF}}(\mathbf{r};[\rho]) & q \gg 1. \end{cases} \tag{28}$$

Since $V_{\mathrm{TF}}(\mathbf{r};[\rho])$ and $V_{\mathrm{W}}(\mathbf{r};[\rho])$ are the only components up to second order of the two exact limiting forms of the KP, we can combine them in analogy to the TFλW and WλTF models and arrive at generalized KPs.

However, instead of combining them using a fixed parameter λ, it seems natural to represent them in Fourier space and allow a wave-vector dependence in $\lambda=\lambda(q)$ to connect the limiting forms. The $\lambda(q)$ can then be chosen in a very simple way so that the exact LR function is reproduced for a uniform system with density ρ_0. In this way the LR function bridges the exact limits at large and small wave vectors, and if the theory is applied to weak perturbations in the linear response regime for intermediate wave vectors, we can expect very accurate results. Here, we derive such generalized KPs based on the KP for the WλTF model.

C. HQ kinetic potential

In analogy to the WλTF model in Eq. (27) we look for a kinetic potential of the form

$$V^0_{\mathrm{HQ}}(\mathbf{k}) = V_{\mathrm{W}}(\mathbf{k}) + \lambda_{\mathrm{HQ}}(q)V_{\mathrm{TF}}(\mathbf{k}) = V_{\mathrm{TF}}(\mathbf{k}) + V_{\mathrm{W}}(\mathbf{k}) + \hat{f}(q)V_{\mathrm{TF}}(\mathbf{k}), \tag{29}$$

where

$$q = k/2k_F \tag{30}$$

is a dimensionless wave vector normalized by the FWV k_F in Eq. (22) of a uniform reference system with density ρ_0 and $\hat{f}(q)=\lambda_{\mathrm{HQ}}(q)-1$. The superscript 0 in V^0_{HQ} indicates use of a uniform reference system. For a small perturbation, we can linearize the $V^0_{\mathrm{HQ}}(\mathbf{k})$ in Eq. (29). Requiring that it satisfy LR exactly then determines the weight function $\hat{f}(q)$ as

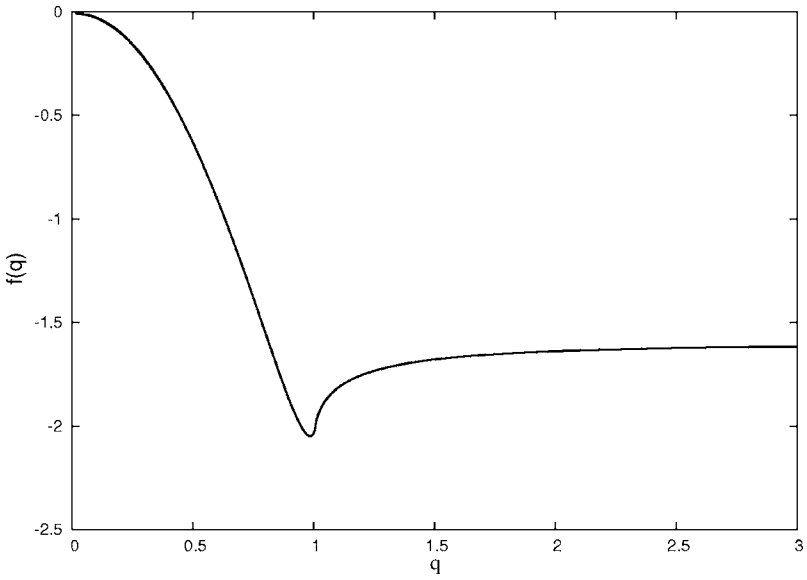

FIG. 2. Weight function $\hat{f}(q)$ for the HQ and LQ KPs.

$$\hat{f}(q) = F_L(q) - 3q^2 - 1. \tag{31}$$

See Fig. 2.

We refer to Eq. (29) with Eq. (31) as the HQ KP model. It reproduces the correct high-q limit in Eq. (28) up to the second order. However, unlike Eq. (16), it also satisfies the correct low-q limit to leading order and gives exact results for all q in the linear response regime. Inverse Fourier transform of Eq. (29) then gives

$$V^0_{\mathrm{HQ}}(\mathbf{r};[\rho],k_F) = V_{\mathrm{TF}}(\mathbf{r};[\rho]) + V_{\mathrm{W}}(\mathbf{r};[\rho]) + \int f(|\mathbf{r}-\mathbf{r}'|;k_F)V_{\mathrm{TF}}(\mathbf{r}';[\rho])d\mathbf{r}'. \tag{32}$$

This expression is directly useful for extended systems where a reasonable ρ_0 can be defined. For isolated systems such as atoms and molecules where the density vanishes far from the nuclei, it seems natural to replace k_F in Eq. (32) by the *local* Fermi wave vector (LFWV),

$$k_F(\mathbf{r}) \equiv [3\pi^2\rho(\mathbf{r})]^{1/3}, \tag{33}$$

though errors may be introduced for rapidly varying density distributions. Using Eq. (13), this yields the general form of our proposed HQ kinetic potential,

$$V_{\mathrm{HQ}}(\mathbf{r};[\rho],k_F(\mathbf{r})) = V_{\mathrm{TF}}(\mathbf{r};[\rho]) + V_{\mathrm{W}}(\mathbf{r};[\rho]) + \frac{5}{3}C_F\int f(|\mathbf{r}-\mathbf{r}'|;k_F(\mathbf{r}))\rho^{2/3}(\mathbf{r}')d\mathbf{r}'. \tag{34}$$

Note that the last term in Eq. (34) is most easily computed in Fourier space as

$$\frac{5C_F}{3(2\pi)^3}\int \hat{f}[k/2k_F(\mathbf{r})]\rho^{2/3}(\mathbf{k})e^{-i\mathbf{k}\cdot\mathbf{r}}d\mathbf{k}. \tag{35}$$

As can been seen in Eq. (31), the weight function $\hat{f}[k/2k_F(\mathbf{r})]$ is determined analytically. Unlike the LR-based KEDF approaches, no first-order differential equation is needed to solve for the weight function in Fourier space. For atomic systems where the LFWV is used, the convolution in Eq. (35) must be carried out numerically, which will lead to a quadratic scaling of the HQ model (and the related LQ model described below) in the number N of electrons. For extended systems where one can expand about the local density ρ_0, one can use fast Fourier transforms (FFT's) for a much more efficient computation of this integral.[44]

D. LQ kinetic potential

In analogy to the TFλW model in Eq. (26), we could similarly generate a KP that is accurate to second order at low q while still reproducing the leading term at high q. However this is numerically less useful because the analogue of Eq. (35) involves the Fourier transform of $V_{\mathrm{W}}(\mathbf{r}';[\rho])$, which cannot be simply expressed in terms of the density. Instead, by empirically taking a properly chosen component of the density outside the integral we find that Eq. (34) can be modified to produce a new LQ KP that is accurate to second order at low q and first order at high q,[45]

$$V_{\mathrm{LQ}}(\mathbf{r};[\rho],k_F(\mathbf{r})) = V_{\mathrm{TF}}(\mathbf{r};[\rho]) + V_{\mathrm{W}}(\mathbf{r};[\rho]) + \frac{20}{9}C_F\rho^{1/6}(\mathbf{r}) \times \int f(|\mathbf{r}-\mathbf{r}'|;k_F(\mathbf{r}))\rho^{1/2}(\mathbf{r}')d\mathbf{r}'. \tag{36}$$

Extending these ideas we have constructed a modified KP that satisfies LR everywhere and is accurate to second order at both low and high q.[45] However, the functional form is much more complicated, and little additional accuracy is gained from the improved behavior at very small or very large wave vectors, since all forms use LR to interpolate for intermediate wave vectors, and this is where most errors arise in practice. Thus, we will report results here only for the HQ and LQ models.

TABLE I. Atomic energy E using the KS, LQ, HQ, CAT, and TFλW models in all-electron calculations. MAPE, the mean absolute percentage error (relative to the KS method) of various OF models are given at the bottom of their respective columns.

	KS	LQ	HQ	CAT	TF1/5W	TFW
He	−2.834	−2.565	−2.437	−2.675	−2.911	−1.559
Ne	−128.2	−134.3	−126.6	−126.2	−129.5	−86.40
Ar	−525.9	−545.9	−512.2	−515.1	−526.2	−375.5
Kr	−2750	−2805	−2621	−2712	−2748	−2099
Xe	−7229	−7306	−6844	−7141	−7214	−5701
Be	−14.45	−14.39	−13.64	−14.11	−14.71	−8.699
Mg	−199.1	−207.9	−195.7	−195.2	−200.0	−136.4
C	−37.42	−38.97	−36.85	−37.25	−38.41	−24.01
N	−54.02	−56.71	−53.59	−53.84	−55.39	−35.33
O	−74.47	−78.39	−74.02	−74.08	−76.11	−49.39
Si	−288.2	−300.4	−282.5	−282.2	−288.9	−200.5
P	−339.9	−354.1	−332.7	−332.8	−340.6	−238.3
S	−396.7	−412.8	−387.7	−388.5	−397.3	−279.9
MAPE		4.06%	3.42%	1.82%	1.10%	32.0%

V. RESULTS FOR ATOMS USING THE HQ AND LQ MODELS

For completeness and to compare to earlier work, we first briefly discuss all-electron calculations using the proposed HQ and LQ model KPs and the full atomic potentials. We then describe results using AILPS methods. These are compared with the KS-DFT, the TFλW models, and the CAT model introduced by Chacón, Alvarellos, and Tarazona.[12–14] The CAT model is a LR-based KEDF method, which gives some indication of shell structure. We employed the latest version, which uses a nonlocal two-body Fermi wave vector with a prescribed functional form depending on an empirical parameter $\beta=1/2$ [defined in Eq. (3) of Ref. 14]. This caused the numerical calculations[46] to be considerably more costly than those of the LQ or HQ models, which used the local Fermi wave vector as in Eq. (33). All calculations are spin-restricted and use the local density approximation (LDA)[47–49] for the exchange-correlation functional.

A. All-electron calculations

All-electron calculations consider the density response to the large and rapidly varying nuclear potential. Since the system is far from the linear response regime, quantitative results from the HQ and LQ models (or from LR-based KEDF methods) cannot be expected. However, by incorporating exact results for very large and very small wave vectors, these models do correct major deficiencies of the purely local TF model (which, e.g., predicts an infinite density at the nucleus) and even give some qualitative indications of atomic shell structure.

The numerical method use the Pauli kinetic potential $V^P(\mathbf{r};[\rho])$,[50,51] defined as

$$V^P(\mathbf{r};[\rho]) \equiv V_{T_s}(\mathbf{r};[\rho]) - V_{\mathrm{W}}(\mathbf{r};[\rho]). \quad (37)$$

Since $V_{\mathrm{W}}(\mathbf{r};[\rho])$ is the exact KP for a system where the density can be accurately described by a single orbital, if $V^P(\mathbf{r};[\rho])$ is omitted, one would essentially obtain the ground-state density of the corresponding boson system, where all the electrons are in the same orbital. If we represent the full density by a single orbital function $\psi(\mathbf{r})$, so that $\rho(\mathbf{r})$ and $V_{\mathrm{W}}(\mathbf{r};[\rho])$ can be written in the forms of Eq. (18) and Eq. (19), respectively, we can then combine $V^P(\mathbf{r};[\rho])$ with the one-body potential $V_{\mathrm{eff}}(\mathbf{r};[\rho])$ in Eq. (3), and derive a Schrödinger-type equation for the Bose orbital $\psi(\mathbf{r})$,

$$\left\{-\tfrac{1}{2}\nabla^2 + V_{\mathrm{eff}}(\mathbf{r};[\rho]) + V^P(\mathbf{r};[\rho])\right\}\psi(\mathbf{r}) = \mu\psi(\mathbf{r}). \quad (38)$$

In other words, $V_{\mathrm{eff}}(\mathbf{r};[\rho])+V^P(\mathbf{r};[\rho])$ is now the one-body effective potential for the corresponding boson system with the same electron density. This reduction of an N-fermion problem to a boson form is widely implemented in OF-DFT due to its numerical stability and its easy implementation using existing KS-DFT codes.[10]

The associated Pauli potentials for the HQ and LQ models are immediately obtained by subtraction of the W KP from Eq. (34) and Eq. (36), respectively. The standard finite difference method for solving Euler equations for the TFW models[52] are implemented for the LQ and HQ models, and the nonlocal terms are evaluated by Fourier transforms. The choices of radial grids for both of the real and Fourier space and other detailed numerical methods are given in Ref. 7. The kinetic energy for HQ and LQ models is computed using the Herring pathway in Eq. (8).

As shown in Table I, the atomic energy calculated by the energy-optimized TF1/5W model is very close to the KS-DFT, and outperforms all the LR-based models, and other TFλW models. In Table II, we compare the electron density at the nucleus $\rho(0)$ for various models. The TF1/5W model overestimates $\rho(0)$ by about a factor of 4, while the TFW model underestimates it by about 30%. The predicted values of $\rho(0)$ for all the LR-based models are very close to the KS results, and are much better than the TFλW models.

TABLE II. Electron density at the nucleus $\rho(0)$, using the KS, LQ, HQ, CAT, and TFλW models in all-electron calculations. MAPE, the mean absolute percentage error (relative to the KS method) of various OF models are given at the bottom of their respective columns.

	KS	LQ	HQ	CAT	TF1/5W	TFW
He	3.525	3.088	2.742	3.600	18.23	0.9515
Ne	614.5	576.6	517.6	613.2	2596	169.6
Ar	3819	3642	3282	3812	1.548×10^4	1093
Be	34.86	30.49	27.17	33.75	158.2	8.952
Mg	1086	1024	920.9	1083	4519	303.0
C	126.0	113.3	101.2	122.8	547.9	33.07
N	203.9	185.6	166.1	200.0	876.7	54.24
O	308.6	284.1	254.6	304.6	1317	83.19
Si	1754	1662	1495	1749	7218	493.9
P	2173	2062	1857	2167	8901	614.5
S	2654	2523	2272	2647	1.083×10^4	753.5
MAPE		7.61%	17.2%	1.14%	331%	72.6%

In Fig. 3, we compare the radial density distribution $r^2\rho(r)$ of the LQ and HQ models to that predicted by other theories for the Kr atom. Both the TF1/5W and TFW models predict smooth and structureless radial density profiles. Using the full Coulombic potential, all the LR-based models can predict an incipient shell structure for heavy atoms ($Z \gtrsim 30$), and these results are typical. Since the potential is certainly far beyond the LR regime, these qualitative results with some suggestion of shell structure are about as good as could be hoped for. The surprisingly good total energies given in Table I for the TF1/5W model and the LR-based models shows that averaged thermodynamic properties are less sensitive to errors in the KP than is the density profile. The difference in the results for the LQ, HQ, and CAT models indicates that the LR-based OF theory is being used outside its range of validity. As shown below, we gain a significant improvement by using the AILPS to deal with these difficulties.

B. *Ab initio* local pseudopotential calculations

As discussed earlier, the use of pseudopotentials in nonlocal LR-based OF-DFT can improve the accuracy of the theory because the weaker pseudopotential is more nearly in the LR regime, where the theory is designed to be accurate. Our proposed HQ and LQ models can be used with any existing AILPS. However, since we want to assess the performance of these models for a wide class of atomic systems, we describe here a method for determining reasonable AILPS for general atomic systems. These pseudopotentials will be used in all our calculations and can be transfered to other molecular and solid-state environments, but we expect (and find in cases where comparison can be made) little change if other reasonable AILPS are used.

Because of the one-to-one mapping between the effective one-body potential acting on a system of N electrons and the electron density in the ground-state configuration, it is possible to obtain a unique local one-body potential that gener-

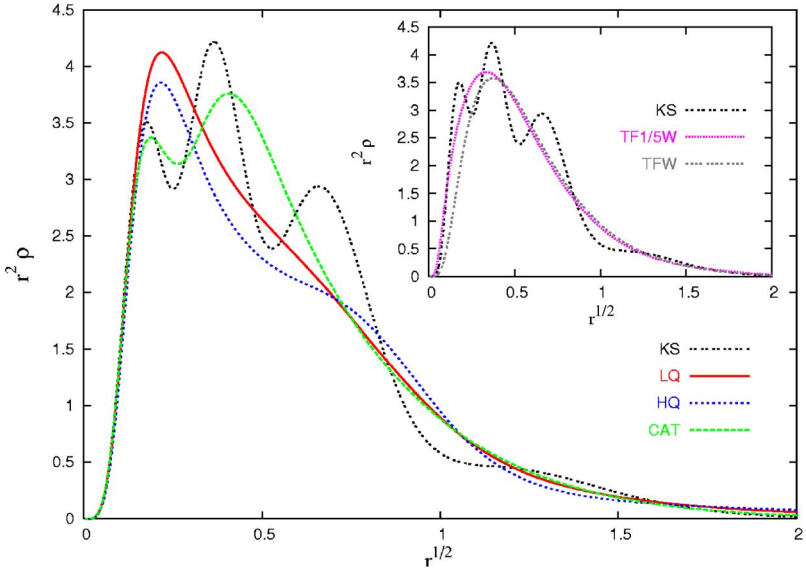

FIG. 3. (Color online) Radial density $r^2\rho(r)$ of the Kr atom using the KS method, the LQ and HQ models, the CAT model, and the TFλW models (see the inset) with the full nuclear potential.

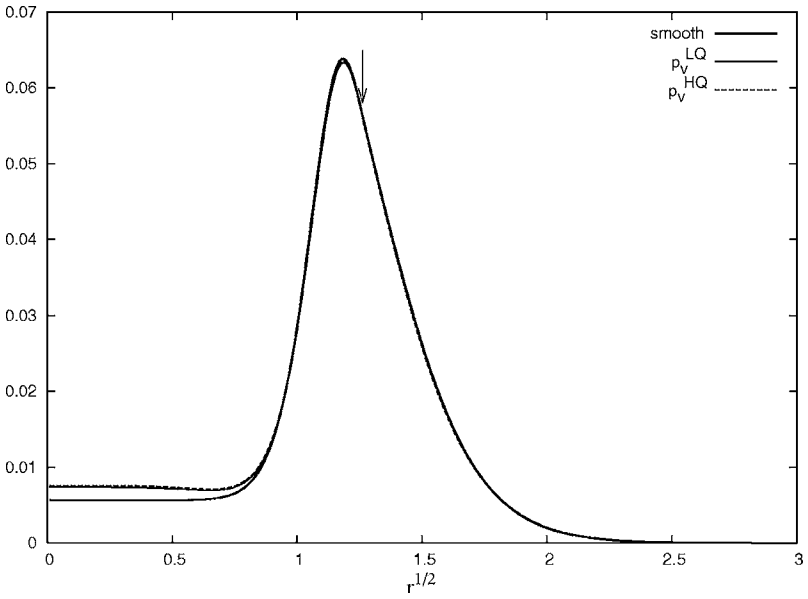

FIG. 4. The smooth target density $\tilde{\rho}_v(r)$ from Eq. (40), with parameters given in Table IV for the Si pseudoatom used in the inverse-KS process, and the valence density $\rho_v(r)$ predicted by the LQ and HQ models using the $V_{ps}(r)$ (see Fig. 5) corresponding to $\tilde{\rho}_v(r)$. The arrow indicates the location of r_c.

ates a given target density $\tilde{\rho}(\mathbf{r})$ by using a KS orbital-based method in an inverse way.[23] To construct an AILPS for a given atom we separate the total electron density $\rho(\mathbf{r})$ into a "core density" $\tilde{\rho}_c(\mathbf{r})$, which is supposed not to vary significantly in other molecular or solid-state environments, and the target "valence density" $\tilde{\rho}_v(\mathbf{r})$ where

$$\rho(\mathbf{r}) = \tilde{\rho}_v(\mathbf{r}) + \tilde{\rho}_c(\mathbf{r}). \tag{39}$$

Because DFT requires only the electron density, we can take a more general view of what is meant by the core and valence components than is used in most orbital-based methods. Here, we directly construct a smooth target valence density for the $N_v = N - N_c$ valence electrons, with N_c chosen to be the number of electrons in the noble gas configuration.

Our proposed target valence density $\tilde{\rho}_v(r)$ for atoms equals the full KS density $\rho_{KS}(r)$ outside a core of radius r_c, and is designed to be small and slowly varying inside r_c. The functional form we take is

$$\tilde{\rho}_v(r) = \begin{cases} t\rho_{KS}(r_c) + a_0 r^q \exp[-r^p(a_1 + a_2 r^2)], & r \leqslant r_c, \\ \rho_{KS}(r), & r > r_c. \end{cases} \tag{40}$$

Figure 4 gives an example of $\tilde{\rho}_v(r)$ for Si that will be discussed in more detail below. We find most results are insensitive to the details of our fitting procedure. Parameter values for a variety of atomic systems are given in Table IV of the Appendix, along with the physical and technical considerations that guided our choice of this particular form for $\tilde{\rho}_v(r)$. The Appendix also discusses some of the general issues that arise in using these atomic AILPS in other environments.

The local pseudopotential is directly related to the effective one-body potential that reproduces $\tilde{\rho}_v(\mathbf{r})$ exactly when using the full KS theory. Following previous work,[24,25] for a given $\tilde{\rho}_v(\mathbf{r})$, the inverse-KS equations are solved to get the effective one-body screened potential $V_{scr}(\mathbf{r})$. The desired *ab initio* local pseudopotential $V_{ps}(\mathbf{r})$ is then obtained by sub-

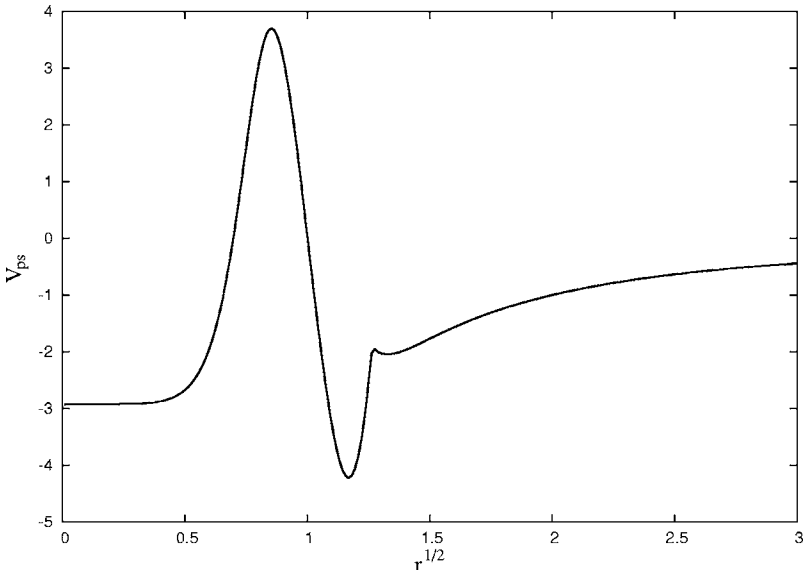

FIG. 5. The AILPS $V_{ps}(r)$ for Si generated by the target density $\tilde{\rho}_v(r)$ in Fig. 4.

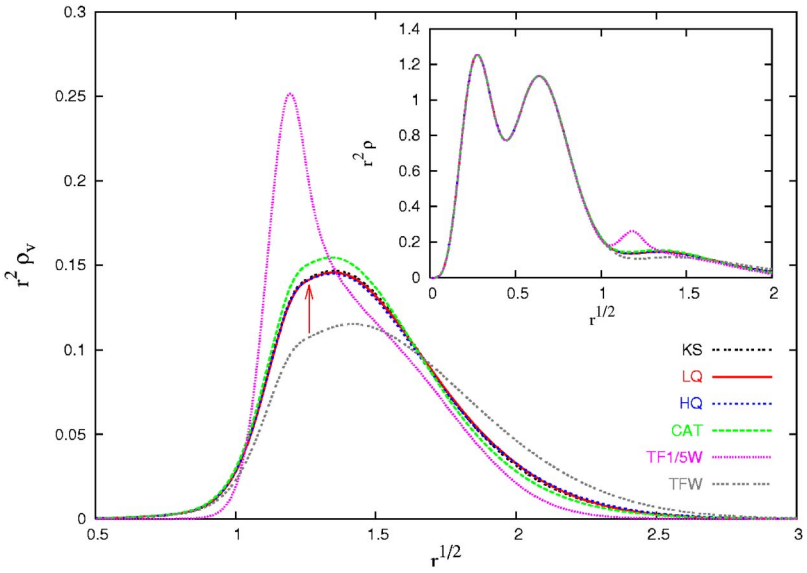

FIG. 6. (Color online) Radial valence density $r^2\rho_v(r)$ of the Si atom using the KS method and various models using AILPS. Parameters used for constructing this reference system are shown in Table IV. The arrow indicates the location of r_c. Inset: The corresponding radial total density $r^2\rho(r)$, which is dominated by the core component for $r<r_c$.

tracting the Hartree potential and the exchange-correlation potential,

$$V_{\rm ps}(\mathbf{r}) = V_{\rm scr}(\mathbf{r}) - V_H(\mathbf{r};[\tilde{\rho}_v]) - V_{\rm xc}(\mathbf{r};[\tilde{\rho}_v]). \quad (41)$$

This relatively expensive procedure to determine $V_{\rm ps}(\mathbf{r})$ requires the use of orbitals. However, it needs to be done only once for each atom, and the resulting $V_{\rm ps}(\mathbf{r})$ can then be used in a variety of other environments if the atomic core densities remain essentially constant.

Once suitable $V_{\rm ps}(\mathbf{r})$ have been determined (by this or other means), they can be incorporated in $V_{\rm ext}(\mathbf{r})$ in different ways, depending on the particular system of interest. OF-DFT theory can then be used to determine the valence density $\rho_v(\mathbf{r})$ in direct analogy to the all-electron calculations for the full atomic potential in Eq. (38),

$$\left\{-\tfrac{1}{2}\nabla^2 + V_H(\mathbf{r};[\rho_v]) + V_{\rm xc}(\mathbf{r};[\rho_v]) + V_{\rm ext}(\mathbf{r}) + V_P(\mathbf{r};[\rho_v])\right\}\psi_v(\mathbf{r}) = \mu\psi_v(\mathbf{r}), \quad (42)$$

where

$$\rho_v(\mathbf{r}) = |\psi_v(\mathbf{r})|^2. \quad (43)$$

A simple and direct test of OF-DFT is to use Eqs. (42) and (43) for the same atomic system for which $V_{\rm ps}(\mathbf{r})$ was constructed. Thus, we take $V_{\rm ext}(\mathbf{r})=V_{ps}(\mathbf{r})$ for a given atom as input data in Eq. (42). The valence density $\rho_v(\mathbf{r})$ predicted by the OF KPs is determined from Eqs. (42) and (43), and can be directly compared to the exact target density $\tilde{\rho}_v(\mathbf{r})$ for this atomic system given by the full KS theory.

This is illustrated in Fig. 4, which shows the input target valence density $\tilde{\rho}_v(r)$ for Si used in the inverse-KS process. The total KS density $\rho_{\rm KS}(r)$ equals $\tilde{\rho}_v(r)$ for $r \geqslant r_c$, indicated by the arrow in Fig. 4, and then increases rapidly for $r<r_c$, reaching a very large value at the nucleus, $\rho_{\rm KS}(0)=1754$. In contrast, the proposed target valence density $\tilde{\rho}_v(r)$ remains small and relatively slowly varying inside the core, with $\tilde{\rho}_v(0)=0.005\,621$.

Also shown in Fig. 4 are the predicted valence densities $\rho_v(r)$ for Si given by the LQ and HQ models. Because of the relatively weak $V_{\rm ps}(r)$ and slowly varying valence density,

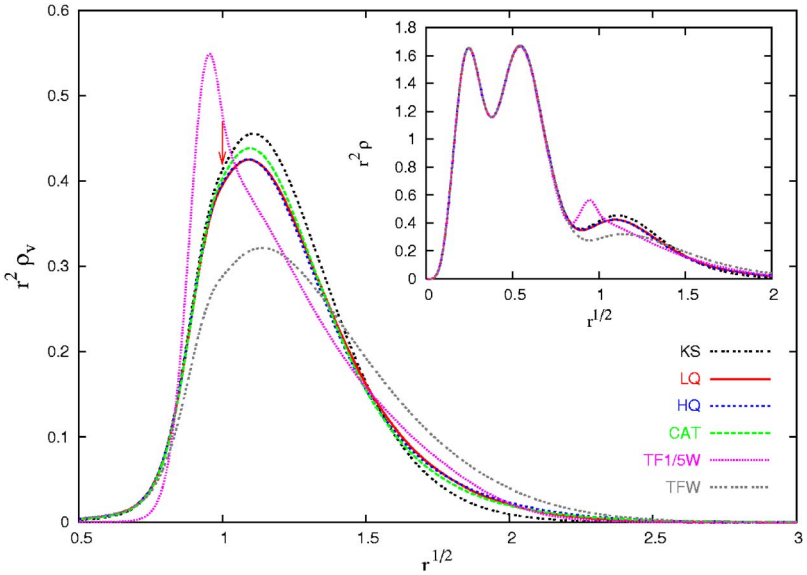

FIG. 7. (Color online) Same as in Fig. 6 but for the Ar atom.

TABLE III. The total valence energy $E_v[\rho_v]$ using the KS method, the LQ and HQ models, the CAT model, and the TFλW models. MAE, the mean absolute error (relative to the KS method) of various OF models are given at the bottom of their respective columns. Parameters used in Eq. (40) for such systems are given in Table IV.

	KS	LQ	HQ	CAT	TF1/5W	TFW
Be	−0.9914	−0.8955	−0.8950	−0.9583	−1.214	−0.7786
C	−6.134	−6.080	−6.100	−6.345	−7.761	−5.266
N	−11.04	−11.06	−11.09	−11.32	−13.93	−9.462
O	−18.01	−18.09	−18.09	−18.19	−22.44	−15.30
Si	−3.771	−3.738	−3.750	−3.869	−4.467	−3.350
P	−6.474	−6.432	−6.455	−6.582	−7.385	−5.756
S	−10.20	−10.10	−10.14	−10.24	−11.27	−9.023
Ar	−21.37	−20.84	−20.91	−20.85	−22.40	−18.56
MAE		0.119	0.103	0.184	1.610	1.312

both the LQ and HQ KP models predict results very close to those given by the exact KS treatment of the kinetic energy, and perform markedly better than they did for the all-electron calculations using the full Coulomb potential. Figure 5 shows the corresponding AILPS generated by the inverse KS procedure. It is much smaller in the core region than the full atomic potential and more likely to be accurately treated by LR-based methods.

The radial valence density $r^2\rho_v(r)$ of the Si and Ar atoms predicted by the various methods are shown in Figs. 6 and 7. The consistency of our OF theory when pseudopotentials are used is illustrated by the similarity of the density predicted by the HQ and LQ models. The slight deviations from the KS-DFT results for Ar in the valence region in Fig. 7 are among the largest we encountered for all atoms tested, and could be due to the relatively large number of valence electrons (8) compared to core electrons (10). Further errors may arise from the LFWV approximation in Eq. (33).

Once $\rho_v(\mathbf{r})$ has been determined using OF-DFT, it can be added to the known input core density $\tilde{\rho}_c(\mathbf{r})$ to obtain the predicted total density, since the basic assumption of our AILPS is that the core density remains unchanged in different chemical environments. The core density is defined in Eqs. (39) and (40). The inset in Fig. 6 shows that the HQ and LQ treatment of the valence density for the Si atom does not produce noticeable errors in the total density, as expected, and the shell structure remains in excellent agreement with the full KS-DFT calculations.

As a further test of OF-DFT, we can compare the energy for the valence density given by the various methods to the exact valence energy for the target valence density determined by the inverse KS method. Table III gives the valence energy values for the KS-DFT, and the LQ and the HQ models. As can been seen, both the LQ and HQ models give very good agreement with KS-DFT and perform significantly better than the other models. These results show that for this class of relatively weak pseudopotentials the OF treatment of the KP is quite satisfactory.

To test the transferability of the present AILPS, we also performed calculations for positive ions. Figure 8 shows that the ionization energies of various atoms calculated using KS-

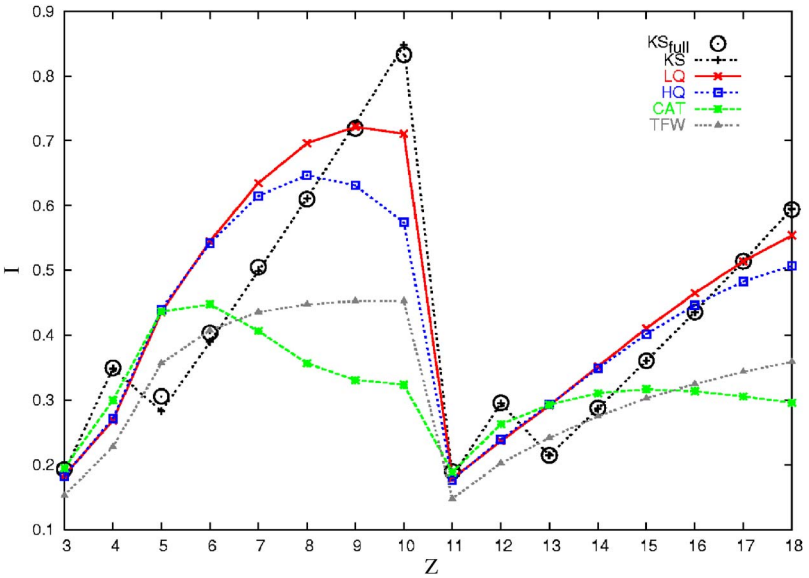

FIG. 8. (Color online) Ionization energies (shown in hartree) of the first and the second row atoms using the full KS method, and various models using AILPS. The mean absolute errors (relative to the full KS method) of various models using AILPS are KS (0.1 eV), LQ (1.8 eV), HQ (2.1 eV), CAT (3.9 eV), TFW (3.1 eV), and TF1/5W (4.3 eV). Ionization energies using the TF1/5W model are not shown in the figure due to its relatively poor performance.

DFT and the full atomic densities and those from the KS-DFT using the valence densities with AILPS are very similar. Therefore, the present AILPS are quite transferable to these positive ions.

The ionization energy for models using the AILPS is obtained by subtracting the valence energies for systems with N_v and N_v-1 electrons. Since the core electrons are assumed to be unaltered in different chemical environments, the atomic core energy is a constant that cancels here or in other similar applications to molecules and solids. Limitations of the LQ and HQ models are more evident here, but they do capture the overall periodicity of the ionization energies well, and perform significantly better than the other models.

VI. CONCLUSION

In summary, we propose two nonlocal OF KPs that satisfy exact limits for small and large wave-vector perturbations and reproduce the exact LR function in the homogeneous limit. These are the same limits that several current KEDFs are designed to satisfy. However, because of the more local nature of the KP, it is much easier to satisfy these conditions for the KP than for the KEDF, and there may be other physical and technical advantages arising from the use of the more local KP.

In general, there is no reason to believe that any LR-based OF-DFT should work well for arbitrary systems where the model potentials are far beyond the LR regime. However, most chemical processes involve changes of valence electron densities, which can often be described by a weak AILPS. Thus, the use of a LR-based OF-KP together with AILPS for atomic systems at least seems well justified. The small and relatively slowly varying $\rho_v(r)$ also provides some justification for our use of the local FWV $k_F(\mathbf{r})$ in Eq. (33).

When the AILPS is used, the valence densities given by the LQ and HQ KPs are close to those given by the KS method. Thus the particular integration pathway used to get the total energy value becomes unimportant. The simple pathway in Eq. (8) is especially useful, since no coupling parameter integration is needed.

The proposed models are not only conceptually simple, but also exact for a model system with a weak potential and a slowly varying density. The appearance of the atomic shell structure was found to be very sensitive to the accuracy of the proposed KPs. The LR-based LQ and HQ KPs give at best only qualitative indications of shell structure for full atomic systems, though total energies are surprisingly good. Still better results for atoms and ions can be found by focusing on the valence density as determined by a relatively weak AILPS. While these results seem promising, improved KPs are needed and further investigation is required to see if these ideas can be usefully applied to other relevant systems like molecules and solids. Some initial results along these lines will be reported elsewhere.

ACKNOWLEDGMENTS

This work has been supported by the NSF Grant No. CHE01-11104, and by the NSF-MRSEC at the University of Maryland under Grant No. DMR 00-80008. One of the authors (J.D.C.) acknowledges the support from the UMCP Graduate School program, the IPST Alexander program, and the CHPH Block Grant Supplemental program. The authors are grateful to Emily Carter and members of her group for many helpful discussions and comments on an earlier version of this paper.

APPENDIX: *AB INITIO* LOCAL PSEUDOPOTENTIALS

As discussed above, our proposed target valence density for atoms has the following form:

$$\tilde{\rho}_v(r) = \begin{cases} t\rho_{\mathrm{KS}}(r_c) + a_0 r^q \exp[-r^p(a_1 + a_2 r^2)], & r \leqslant r_c, \\ \rho_{\mathrm{KS}}(r), & r > r_c. \end{cases} \tag{A1}$$

Here p and q are taken as even integers. The larger they are, the smaller and more slowly varying is the valence density near $r=0$ but the sharper is the peak near the core radius r_c. As a compromise, we take here $p=q=6$, which generates relatively slowly varying local pseudopotentials $V_{\mathrm{ps}}(r)$. For applications in different environments, such as molecules or crystals, the core size r_c must be small to maintain transferability of the atomic core density. For this reason, we force $\tilde{\rho}_v(r=0)$ to be small by taking a small t. If $t=0$, the strict vanishing of the valence density near the nucleus would require a very repulsive V_{ps}, which is certainly undesirable for the LR-based OF-DFT. However, if t is too large, there will exist a long oscillatory tail outside the core in the corresponding $V_{\mathrm{ps}}(r)$. This is an undesirable feature for transferability to other environments, as will be discussed below. These two points constrain the value of t and we use here $t=0.1$ for all the atomic systems considered.

The four parameters a_0, a_1, a_2, and r_c are determined by requiring continuity of the function $\tilde{\rho}_v(r)$ and its first two derivatives at $r=r_c$, and by satisfying the normalization condition

$$N_v = 4\pi \int \tilde{\rho}_v(r) r^2 dr. \tag{A2}$$

Here we used the standard noble gas cores to determine $N_v = N - N_c$, though other choices could in principle be made. See Table IV for values of the parameters used in Eq. (A1).

To construct our local pseudopotential $V_{\mathrm{ps}}(r)$ for atoms, we first solve the KS equations for an atom with the full Coulomb potential. With the KS density $\rho_{\mathrm{KS}}(r)$ and N_c determined, this construction ensures that as $r \to r_c$, the associated core density smoothly approaches zero as $O(|r-r_c|^3)$.

After generating the parametrized target valence density $\tilde{\rho}_v(r)$, the set of inverse-KS equations are solved to obtain the corresponding one-body screened potential $V_{\mathrm{scr}}(r)$. In principle, the AILPS $V_{\mathrm{ps}}(r)$ is then given by Eq. (41). Using this, we find with an acceptable N_c that essentially the same density profiles outside r_c are predicted by the LQ and HQ models for a wide range of choices of p, q, and t. This would be expected if most features of the resulting set of model potentials are within the different regimes accurately described by the OF KP. These results clearly show that OF-DFT can give

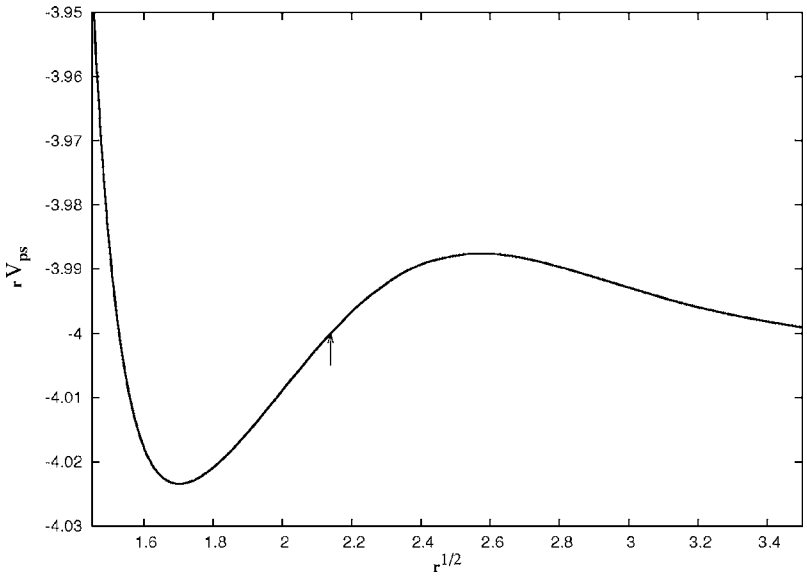

FIG. 9. The inverse KS procedure generates very small oscillations in the tail of $rV_{ps}(r)$ for Si (shown here) and other atoms. The two points where $rV_{ps}(r)=-4$ for Si are $r_1=2.336$ and $r_2=4.576$ or $r_2^{1/2}=2.139$. The arrow indicates the location of r_2. To achieve good transferability (see text), this $rV_{ps}(r)$ is modified by setting $rV_{ps}(r)=-4$ when $r \geqslant r_2=4.576$. See Fig. 5 for a large scale view.

accurate results for this class of physically relevant and relatively weak and slowly varying model potentials.

However, we found that the $rV_{ps}(r)$ constructed in this way for group III to group VIII elements deviates from $-Z_v$ outside the core by a small and long range oscillation. For the $2s^2 2p^x$ atoms, the maximum amplitude of the oscillation is about 0.18. For the $3s^2 3p^x$ atoms, it ranges from 0.003 for Al to 0.037 for Ar. Similar oscillatory tails were observed by Wang and Stott,[25] and are thought to arise from the inability of a local pseudopotential to represent both s and p orbitals of the corresponding nonlocal pseudopotentials. These oscillations are so small in magnitude that they have almost no effect on the density profile or energy of atoms, but they can cause transferability problems when used for solids.[53] Following the Wang and Stott approach, we replace $V_{ps}(r)$ by $-Z_v/r$ at the largest point where $rV_{ps}(r)=-Z_v$ [see Fig. 9]. The new $V_{ps}(r)$ can then be used for both atomic and solid-state calculations.

In other chemical environments, such molecules and solids, the predetermined AILPS $V_{ps}(\mathbf{r})$ centered at each nucleus are regarded as input data, and the valence densities for other systems can be calculated by OF-DFT. Results can be checked by using the full KS-DFT. For example, for molecules and solids, the external potential $V_{ext}(\mathbf{r})$ is a linear

TABLE IV. Parameters used in Eq. (A1) for the target valence density of various atoms. Here, $p=q=6$, and $t=0.1$ are used for all systems. The $V_{ps}(r)$ generated from these parametrized $\tilde{\rho}_v(r)$ can then be used in OF-DFT.

	N_v	a_0	a_1	a_2	r_c
Li	1	2.983×10^{-4}	0.05260	-6.560×10^{-3}	2.135
Be	2	0.02655	0.7078	−0.2130	1.370
B	3	0.8032	5.855	−3.531	0.9714
C	4	11.53	30.17	−31.20	0.7429
N	5	98.80	112.8	−180.2	0.5978
O	6	592.7	338.9	−779.8	0.4981
F	7	2750	871.4	−2744	0.4256
Ne	8	1.052×10^{4}	1993	−8267	0.3707
Na	1	5.234×10^{-5}	9.840×10^{-3}	-6.610×10^{-4}	2.904
Mg	2	9.805×10^{-4}	0.04445	-5.002×10^{-3}	2.233
Al	3	6.164×10^{-3}	0.1273	−0.02056	1.861
Si	4	0.02942	0.3119	−0.06861	1.593
P	5	0.1149	0.6864	−0.1979	1.390
S	6	0.3841	1.390	−0.5100	1.231
Cl	7	1.133	2.632	−1.201	1.103
Ar	8	3.018	4.714	−2.624	0.9985

combination of the local atomic pseudopotentials centered at each ion position $\mathbf{R}_I$,

$$V_{\text{ext}}(\mathbf{r}) = \sum_I V_{\text{ps}}(\mathbf{r} - \mathbf{R}_I). \tag{A3}$$

The valence density can then be determined from Eqs. (42) and (43), and the total energy of valence electrons is

$$E_v[\rho_v] = T_s[\rho_v] + E_H[\rho_v] + E_{\text{xc}}[\rho_v] + \int \rho_v(\mathbf{r}) V_{\text{ext}}(\mathbf{r}) d\mathbf{r}. \tag{A4}$$

For the proposed LQ and HQ KPs, the value of $T_s[\rho_v]$ in Eq. (A4) is determined by Eqs. (8) or (11) with $\rho(\mathbf{r})$ replaced by $\rho_v(\mathbf{r})$.

*Electronic address: jdchai@berkeley.edu. Present address: Molecular Foundry, Materials Sciences Division, Lawrence Berkeley National Laboratory, and Department of Chemistry, University of California, Berkeley, California 94720.

[1] P. Hohenberg and W. Kohn, Phys. Rev. **136**, B864 (1964).
[2] R. G. Parr and W. Yang, *Density-Functional Theory of Atoms and Molecules* (Oxford University Press, Oxford, 1989).
[3] R. M. Dreizler and E. K. U. Gross, *Density Functional Theory: An Approach to the Quantum Many Body Problem* (Springer-Verlag, Berlin, 1990).
[4] W. Kohn and L. J. Sham, Phys. Rev. **140**, A1133 (1965).
[5] L. J. Sham and W. Kohn, Phys. Rev. **145**, 561 (1966).
[6] R. A. King and N. C. Handy, Phys. Chem. Chem. Phys. **2**, 5049 (2000); Mol. Phys. **99**, 1005 (2001).
[7] J.-D. Chai and J. D. Weeks, J. Phys. Chem. B **108**, 6870 (2004).
[8] Y. A. Wang, N. Govind, and E. A. Carter, Phys. Rev. B **58**, 13465 (1998).
[9] Y. A. Wang, N. Govind, and E. A. Carter, Phys. Rev. B **60**, 16350 (1999).
[10] See e.g., Y. A. Wang and E. A. Carter, "Theoretical methods in condensed phase chemistry," in *Progress in Theoretical Chemistry and Physics*, edited by S. D. Schwartz (Kluwer, Boston, 2000), p. 117, and references therein.
[11] B. Zhou, V. L. Ligneres, and E. A. Carter, J. Chem. Phys. **122**, 044103 (2005).
[12] E. Chacón, J. E. Alvarellos, and P. Tarazona, Phys. Rev. B **32**, 7868 (1985).
[13] P. García-González, J. E. Alvarellos, and E. Chacón, Phys. Rev. A **54**, 1897 (1996).
[14] P. García-González, J. E. Alvarellos, and E. Chacón, Phys. Rev. B **57**, 4857 (1998).
[15] M. Pearson, E. Smargiassi, and P. A. Madden, J. Phys.: Condens. Matter **5**, 3221 (1993); E. Smargiassi and P. A. Madden, Phys. Rev. B **49**, 5220 (1994); M. Foley and P. A. Madden, *ibid.* **53**, 10589 (1996).
[16] F. Perrot, J. Phys.: Condens. Matter **6**, 431 (1994).
[17] J. A. Alonso and L. A. Girifalco, Phys. Rev. B **17**, 3735 (1978); M. D. Glossman, L. C. Balbás, and J. A. Alonso, Chem. Phys. **196**, 455 (1995).
[18] C. Herring, Phys. Rev. A **34**, 2614 (1986).
[19] L.-W. Wang and M. P. Teter, Phys. Rev. B **45**, 13196 (1992).
[20] N. Choly and E. Kaxiras, Solid State Commun. **121**, 281 (2002).
[21] L. H. Thomas, Proc. Cambridge Philos. Soc. **23**, 542 (1927); E. Fermi, Z. Phys. **48**, 73 (1928).
[22] See e.g., R. Evans, in *Fundamentals of Inhomogeneous Fluids*, edited by D. Henderson (Dekker, New York, 1992), p. 85.
[23] Y. Wang and R. G. Parr, Phys. Rev. A **47**, R1591 (1993).
[24] B. Zhou, Y. A. Wang, and E. A. Carter, Phys. Rev. B **69**, 125109 (2004).
[25] B. Wang and M. J. Stott, Phys. Rev. B **68**, 195102 (2003).
[26] A. Holas and N. H. March, Phys. Rev. A **66**, 066501 (2002); I. Lindgren and S. Salomonson, *ibid.* **67**, 056501 (2003).
[27] L. R. Pratt, G. G. Hoffman, and R. A. Harris, J. Chem. Phys. **88**, 1818 (1988); **92**, 6687 (1990); G. G. Hoffman and L. R. Pratt, Mol. Phys. **82**, 245 (1994).
[28] Y.-G. Chen and J. D. Weeks, J. Chem. Phys. **118**, 7944 (2003).
[29] J. P. Perdew and S. Kurth, in *Density Functionals: Theory and Applications*, edited by D. Joubert, Lecture Notes in Physics (Springer-Verlag, Berlin, 1998) p. 8, and references therein.
[30] L. J. Sham, Phys. Rev. A **1**, 969 (1970).
[31] M. Levy and J. P. Perdew, Phys. Rev. A **32**, 2010 (1985).
[32] F. W. Averill and G. S. Painter, Phys. Rev. B **24**, 6795 (1981).
[33] W. Yang, Phys. Rev. A **34**, 4575 (1986).
[34] C. F. von Weizsäcker, Z. Phys. **96**, 431 (1935).
[35] J. Lindhard, K. Dan. Vidensk. Selsk. Mat. Fys. Medd. **28**, 8 (1954).
[36] W. Jones and W. H. Young, J. Phys. C **4**, 1322 (1971).
[37] Y. Tomishima and K. Yonei, J. Phys. Soc. Jpn. **21**, 142 (1966).
[38] E. H. Lieb, Rev. Mod. Phys. **53**, 603 (1981).
[39] G. K.-L. Chan, A. J. Cohen, and N. C. Handy, J. Chem. Phys. **114**, 631 (2001).
[40] P. K. Acharya, L. J. Bartolotti, S. B. Sears, and R. G. Parr, Proc. Natl. Acad. Sci. U.S.A. **77**, 6978 (1980).
[41] J. L. Gázquez and J. Robles, J. Chem. Phys. **76**, 1467 (1982).
[42] L. J. Bartolotti and P. K. Acharya, J. Chem. Phys. **77**, 4576 (1982).
[43] P. K. Acharya, J. Chem. Phys. **78**, 2101 (1983).
[44] D. J. Singh, Phys. Rev. B **48**, 14099 (1993).
[45] J.-D. Chai, Ph.D. dissertation, University of Maryland, 2005.
[46] Instead of solving the second-order differential equation numerically for the corresponding weight function $\omega(x)$ [see Eq. 14 of Ref. 13], we used the parametrized form in the appendix of Ref. 13. Although the parametrization was made for $\beta=-1/2$ (note the sign change of β in Ref. 13), the β dependence of $\omega(x)$ is small for small β, as argued in Ref. 14. Our results for the CAT model using this parametrized $\omega(x)$ are very close to their reported results.
[47] P. A. M. Dirac, Proc. Cambridge Philos. Soc. **26**, 376 (1930).
[48] D. M. Ceperley, Phys. Rev. B **18**, 3126 (1978); D. M. Ceperley and B. J. Alder, Phys. Rev. Lett. **45**, 566 (1980).
[49] J. P. Perdew and A. Zunger, Phys. Rev. B **23**, 5048 (1981).
[50] N. H. March, Phys. Lett. A **113**, 476 (1986).
[51] A. Holas and N. H. March, Phys. Rev. A **44**, 5521 (1991).
[52] A. M. Abrahams and S. L. Shapiro, Phys. Rev. A **42**, 2530 (1990).
[53] D. M. Bylander and L. Kleinman, Phys. Rev. B **55**, 9432 (1997).